



DESIGN, SYNTHESIS AND MOLECULAR DOCKING OF SOME DERIVATIVES OF 9-METHYLPYRAZOLO[1,5-*d*][1,2,4]TRIAZOLO[3,4-*f*][1,2,4]TRIAZINE-3-THIOL

*BAZI 9-METİLPİRAZOLO[1,5-*d*][1,2,4]TRİAZOLO[3,4-*f*][1,2,4]TRİAZİN-3-TİYOL TÜREVLERİNİN TASARIMI, SENTEZİ VE MOLEKÜLER YERLEŞTİRİLMESİ*

Sergey FEDOTOV^{1*} , Andrey GOTSULYA¹ , Yevhen ZAIKA² ,
Tetiana BRYTANOVA¹ 

¹Zaporizhzhia State Medical University, Faculty of Pharmacy, Department of Natural Sciences for Foreign Students and Toxicological Chemistry, Zaporizhzhia, Ukraine

²Enamine Ltd, Kyiv, Ukraine

ABSTRACT

Objective: *The purpose of the work was to elaboration effective techniques for the synthesis of advanced condensed heterocyclic systems based on pyrazole and 1,2,4-triazole. In the process of realizing the set goal, a number of new pyrazolo[1,5-*d*][1,2,4]triazolo[3,4-*f*][1,2,4]triazines have been synthesized.*

Material and Method: *Identity of synthesized compounds has been confirmed by elemental analysis, ¹H-NMR, LC-MS techniques. The pharmacological potential of the obtained substances has been determined by molecular docking method.*

Result and Discussion: *The optimal conditions for the preparation of pyrazolo[1,5-*d*][1,2,4]triazolo[3,4-*f*][1,2,4]triazines has been determined. Based on the results of molecular docking, a row of substances with high potential for anti-inflammatory and antifungal activity has been identified. In silico studies were carried out using the models of cyclooxygenase-2, lanosta-8,24-dien-3 β -ol 14 α -demethylase, anaplastic lymphoma kinase.*

Keywords: *1,2-Diazole, 1,2,4-triazole, chemistry, molecular docking, transformation*

* **Corresponding Author / Sorumlu Yazar:** Sergey Fedotov
e-mail / e-posta: serjioolegovich@gmail.com, **Phone / Tel.:** +380665837409

Submitted / Gönderilme : 27.09.2022

Accepted / Kabul : 11.01.2023

Published / Yayınlanma : 20.05.2023

ÖZ

Amaç: Çalışmanın amacı, pirazol ve 1,2,4-triazole dayalı gelecek vaat eden kondanse heterosiklik sistemlerin sentezi için etkili yöntemler geliştirmektir. Belirlenen hedefi gerçekleştirme sürecinde, bir dizi yeni pirazolo[1,5-d][1,2,4]triazolo[3,4-f][1,2,4]triazin sentezlenmiştir.

Gereç ve Yöntem: Sentezlenen bileşiklerin yapısı, element analizi, ¹H-NMR, LC-MS teknikleri ile doğrulanmıştır. Elde edilen maddelerin farmakolojik potansiyeli moleküler modelleme yöntemi ile belirlenmiştir.

Sonuç ve Tartışma: Pirazolo[1,5-d][1,2,4]triazolo[3,4-f][1,2,4]triazinlerin hazırlanması için optimal koşullar belirlendi. Moleküler yerleştirme sonuçlarına dayanarak, anti-inflamatuar ve antifungal aktivite için yüksek potansiyele sahip bir dizi madde tanımlanmıştır. Siklooksijenaz-2, lanosta-8,24-dien-3β-ol 14α-demetilaz, anaplastik lenfoma kinazlarının modelleri kullanılarak in siliko çalışmalar yürütülmüştür.

Anahtar Kelimeler: 1,2-Diazol, 1,2,4-triazol, dönüşüm, kimya, moleküler yerleştirme

INTRODUCTION

Organic compounds of heterocyclic nature provide a wide range of opportunities for scientists in the field of medical chemistry. And here, special attention is focused on cycles with Nitrogen [1-4]. Among such compounds, we can note 1,2-diazole and 1,2,4-triazole, as well as derivatives of these structures [5]. Wide possibilities of chemical modification, availability of reagents, high pharmacological potential. It is these factors that determine the choice of research topic in favor of these groups of compounds [6-9]. The combination of these heterocycles within the same structure will contribute to the emergence of new biological properties or enhance existing properties [10,11]. In addition, the choice of heterocyclic system data makes studies of anti-inflammatory, antifungal and anti-cancer activity justified. Such a polypharmacological profile only increases the relevance and practical significance of research related to the creation of polycondensed heterocyclic systems and examine their characteristics.

The aim of the chosen direction of scientific work was to design and synthesize new derivatives of 9-methylpyrazolo[1,5-d][1,2,4]triazolo[3,4-f][1,2,4]triazine, followed by establishing the pharmacological potential of the synthesized number of compounds by computer chemistry methods.

MATERIAL AND METHOD

Chemistry

The first stage of scientific work was represented by the synthetic part. For its implementation, a pyrazole fragment was first constructed. For this purpose, freshly prepared sodium methylate and a mixture of acetone and diethylxalate were used as starting materials (Figure 1) [12,13]. The engagement of these compounds contributed to the creation of an intermediate in the form of ethyl 2,4-dioxopentanoate (1.1). The synthesized compound 1.1 in the reaction of interaction with hydrazine hydrate made it possible to form a hydrazide of formula 1.2. Further, the resulting 5-methylpyrazole-3-carbohydrazide was converted to xanthogenate of formula 1.3 by carbon disulfide in a 9% solution of potassium hydroxide in butan-1-ol. The nature of the subsequent transformation was determined by applying a double amount of hydrazine hydrate, which made it possible to obtain 4-amino-5-(5-methylpyrazol-5-yl)-1,2,4-triazole-3-thiol (2). The presence of SH-group made the alkylation process, which was carried out with the participation of bromoalkanes, convenient. At the last stage of the chemical part of the work, optimal conditions for the reaction of an alkyl-derived thiol of formula 2 with triethoxymethane were established. All chemicals, which mentioned in this work, were obtained from "UKRORGSYNTEZ Ltd" with documental approving of its purity and quality.

Proof of the chemical structure, purity and individuality of chemical conversion products is implemented employing common physical-and-chemical methods of analysis. The melting temperature range was determined by capillary method using SRS Inc MPA 100 equipment. The qualitative composition of the elements and their quantitative ratio were determined using the CHNS analyzer "VarioELcube". Proton-NMR spectroscopy spectra have been received using a Varian Mercury 400

spectrometer (internal standard - tetramethylsilane in dimethylsulfoxide-*d*₆ solution). Chromato-mass spectrometry was performed on the basis of analytical HPLC systems "1260 Infinity" (Agilent), which is equipped with a spectrometer "6120" (Agilent); ionization was performed by spraying in an electric field [15].

Molecular Docking

The second part of the scientific research was related to the preliminary determination of the potential of biological activity using computer simulations. This area of research was implemented using the molecular docking method.

Model enzyme complexes (cyclooxygenase-2, lanosterol 14 α -dimethylase, receptor tyrosine kinase) with standard ligands were loaded from a Protein Data Bank. The choice of these enzymes was dictated by the properties of pharmacophore moiety in a number of target products of the chemical transformation [16,17].

The selection of biotargets were determined by the presence of similar pharmacophore snippets in the structure of substances received along with some known drugs.

Molecular docking was performed in stages. First of all, ligands were prepared, which included: 1) using the software product MarvinSketch-6.3.0 (forming the structure of the studied compounds and saving them in mol format); 2) using the Chem 3D program and a molecular mechanical algorithm, followed by saving the results in pdf files (optimizing the structures of the studied molecules); 3) working in AutoDockTools-1.5.6 and reproducing the results as pdbqt format (adding polar Hydrogen atoms) [18-20].

Then the enzyme was prepared, which included: 1) using the Discovery Studio 4.0 software and then saving the results in pdb format (removing the original ligands and water molecules); 2) using AutoDockTools-1.5.6 (converting the pdb file format to pdbqt). As a result, molecular docking was performed, which included: 1) the use of Vina software (obtaining intermolecular interaction energy values); 2) the use of the AutoDockTools-1.5.6 program (visualization of the results of the study).

RESULT AND DISCUSSION

Chemistry

The path of obtaining target chemical transformation products is shown in Figure 1. Methods for obtaining compounds 1, 1.1, 1.2, and 2 and their basic physico-chemical constants are described in our previous works [12,13]. Substance 1.3 was resynthesized according to the described technique [14]. The main physical and chemical constants of substance 1.3 correspond to known values [14]. The obtaining and characteristics of *S*-alkyl substituted of 4-amino-5-(5-methylpyrazol-3-yl)-1,2,4-triazole-3-thiol (2.1-2.10) were also described in previous work [13]. The final products of chemical conversion (2.12-2.20) were obtained by heating *S*-alkyl derivatives 2.1-2.10 with triethyl orthoformate to a boil for 12 hours.

9-Methyl-3-(alkylthio)pyrazolo[1,5-*d*][1,2,4]triazolo[3,4-*f*][1,2,4]triazine (2.11-2.20)

Compounds 2.1-2.10 (0.01 mol) were placed in a round-bottomed flask, 40 ml of triethyl orthoformate was added and boiled for 12 hours. Excess triethyl orthoformate was removed by low-pressure distillation. The reaction products were recrystallized from propan-2-ol.

9-Methyl-3-(methylthio)pyrazolo[1,5-*d*][1,2,4]triazolo[3,4-*f*][1,2,4]triazine (2.11)

White crystalline solid in 64% yield, m. p. (°C): 212 – 214. ¹H-NMR (400 MHz), δ (ppm): 8.95 (s, 1H, Triazine CH), 7.73 (s, 1H, Pyrazole CH), 2.76 (s, 3H, S-CH₃), 2.45 (s, 3H, CH₃-pyrazole). ESI MS (m/z): [M+H]⁺ at 221. Elemental analysis (EA) (C₈H₈N₆S), calculated, %: C - 43.63, H - 3.66, N - 38.16, S - 14.56; obtained, %: C - 43.74, H - 3.65, N - 38.06, S - 14.60.

3-(Ethylthio)-9-methylpyrazolo[1,5-*d*][1,2,4]triazolo[3,4-*f*][1,2,4]triazine (2.12)

White crystalline solid in 67% yield, m. p. (°C): 186 – 184. ¹H-NMR (400 MHz), δ (ppm): 8.92 (s, 1H, Triazine CH), 7.76 (s, 1H, Pyrazole CH), 3.24 (q, *J*=6.2 Hz, 2H, S-CH₂-CH₃), 2.44 (s, 3H,

Pyrazole-CH₃), 1.32 (t, $J=6.0$ Hz, 3H, S-CH₂-CH₃). ESI MS (m/z): [M+H]⁺ at 234. EA (C₉H₁₀N₆S), calculated, %: C - 46.14, H - 4.30, N - 35.87, S - 13.68; obtained, %: C - 46.02, H - 4.31, N - 35.78, S - 13.71.

9-Methyl-3-(propylthio)pyrazolo[1,5-d][1,2,4]triazolo[3,4-f][1,2,4]triazine (2.13)

White crystalline solid in 81% yield, m. p. (°C): 170 – 172. ¹H-NMR (400 MHz), δ (ppm): 8.94 (s, 1H, Triazine CH), 7.74 (s, 1H, Pyrazole CH), 3.12 (t, $J=5.1$ Hz, 2H, S-CH₂-C₂H₅), 2.45 (s, 3H, Pyrazole-CH₃), 1.78 (q, $J=5.3$ Hz, 2H, S-CH₂-CH₂-CH₃), 1.07 (t, $J=7.0$ Hz, 3H, S-(CH₂)₂-CH₃). ESI MS (m/z): [M+H]⁺ at 249. EA (C₁₀H₁₂N₆S), calculated, %: C - 48.37, H - 4.87, N - 33.85, S - 12.91; obtained, %: C - 48.49, H - 4.88, N - 33.76, S - 12.87.

3-(Butylthio)-9-methylpyrazolo[1,5-d][1,2,4]triazolo[3,4-f][1,2,4]triazine (2.14)

White crystalline solid in 74% yield, m. p. (°C): 179 – 181. ¹H-NMR (400 MHz), δ (ppm): 8.96 (s, 1H, Triazine CH), 7.73 (s, 1H, Pyrazole CH), 3.27 (t, $J=6.7$ Hz, 2H, S-CH₂-C₃H₇), 2.42 (s, 3H, Pyrazole-CH₃), 1.72–1.63 (m, 2H, S-CH₂-CH₂-C₂H₅), 1.41–1.36 (m, 2H, S-(CH₂)₂-CH₂-CH₃), 0.92 (t, $J=7.1$ Hz, 3H, S-(CH₂)₃-CH₃). ESI MS (m/z): [M+H]⁺ at 263. EA (C₁₁H₁₄N₆S), calculated, %: C - 50.36, H - 5.38, N - 32.04, S - 12.22; obtained, %: C - 50.49, H - 5.39, N - 31.95, S - 12.19.

9-Methyl-3-(pentylthio)pyrazolo[1,5-d][1,2,4]triazolo[3,4-f][1,2,4]triazine (2.15)

White crystalline solid in 77% yield, m. p. (°C): 173 – 175. ¹H-NMR (400 MHz), δ (ppm): 8.93 (s, 1H, Triazine CH), 7.76 (s, 1H, Pyrazole CH), 3.28 (t, $J=6.0$ Hz, 2H, S-CH₂-C₄H₉), 2.44 (s, 3H, Pyrazole-CH₃), 1.78–1.74 (m, 2H, S-CH₂-CH₂-C₃H₇), 1.45–1.33 (m, 4H, S-(CH₂)₂-(CH₂)₂-CH₃), 0.93–0.84 (m, 3H, S-(CH₂)₄-CH₃). ESI MS (m/z): [M+H]⁺ at 277. EA (C₁₂H₁₆N₆S), calculated, %: C - 52.15, H - 5.84, N - 30.41, S - 11.60; obtained, %: C - 52.01, H - 5.85, N - 30.48, S - 11.56.

3-(Hexylthio)-9-methylpyrazolo[1,5-d][1,2,4]triazolo[3,4-f][1,2,4]triazine (2.16)

White crystalline solid in 65% yield, m. p. (°C): 188 – 190. ¹H-NMR (400 MHz), δ (ppm): 8.95 (s, 1H, Triazine CH), 7.74 (s, 1H, Pyrazole CH), 3.27 (t, $J=6.4$ Hz, 2H, S-CH₂-C₅H₁₁), 2.42 (s, 3H, Pyrazole-CH₃), 1.69–1.64 (m, 2H, S-CH₂-CH₂-C₄H₉), 1.42–1.30 (m, 2H, S-(CH₂)₂-CH₂-C₃H₇), 1.39–1.26 (m, 4H, S-(CH₂)₃-(CH₂)₂-CH₃), 0.94–0.89 (m, 3H, S-(CH₂)₅-CH₃). ESI MS (m/z): [M+H]⁺ at 291. EA (C₁₃H₁₈N₆S), calculated, %: C - 53.77, H - 6.25, N - 28.94, S - 11.04; obtained, %: C - 53.62, H - 6.24, N - 29.01, S - 11.07.

3-(Heptylthio)-9-methylpyrazolo[1,5-d][1,2,4]triazolo[3,4-f][1,2,4]triazine (2.17)

White crystalline solid in 71% yield, m. p. (°C): 194 – 196. ¹H-NMR (400 MHz), δ (ppm): 8.94 (s, 1H, Triazine CH), 7.75 (s, 1H, Pyrazole CH), 3.28 (t, $J=6.2$ Hz, 2H, S-CH₂-(CH₂)₅-CH₃), 2.45 (s, 3H, Pyrazole-CH₃), 1.67–1.63 (m, 2H, S-CH₂-CH₂-C₅H₁₁), 1.44–1.35 (m, 2H, S-(CH₂)₂-CH₂-C₄H₉), 1.34–1.26 (m, 6H, S-(CH₂)₃-(CH₂)₃-CH₃), 0.93–0.88 (m, 3H, S-(CH₂)₆-CH₃). ESI MS (m/z): [M+H]⁺ at 305. EA (C₁₄H₂₀N₆S), calculated, %: for: C - 55.24, H - 6.62, N - 27.61, S - 10.53; obtained, %: C - 55.11, H - 6.61, N - 27.68, S - 10.56.

9-Methyl-3-(octylthio)pyrazolo[1,5-d][1,2,4]triazolo[3,4-f][1,2,4]triazine (2.18)

White crystalline solid in 63% yield, m. p. (°C): 187 – 189. ¹H-NMR (400 MHz), δ (ppm): 8.96 (s, 1H, Triazine CH), 7.74 (s, 1H, Pyrazole CH), 3.26 (t, $J=6.3$ Hz, 2H, S-CH₂-C₇H₁₅), 2.44 (s, 3H, Pyrazole-CH₃), 1.69–1.64 (m, 2H, S-CH₂-CH₂-C₆H₁₃), 1.40–1.23 (m, 10H, m, 2H, S-(CH₂)₂-(CH₂)₅-CH₃), 0.94–0.89 (m, 3H, S-(CH₂)₇-CH₃). ESI MS (m/z): [M+H]⁺ at 319. EA (C₁₅H₂₂N₆S), calculated, %: C - 56.58, H - 6.96, N - 26.39, S - 10.07; obtained, %: C - 56.43, H - 6.98, N - 26.46, S - 10.04.

9-Methyl-3-(nonylthio)pyrazolo[1,5-d][1,2,4]triazolo[3,4-f][1,2,4]triazine (2.19)

White crystalline solid in 68% yield, m. p. (°C): 186 – 184. ¹H-NMR (400 MHz), δ (ppm): 8.95 (s, 1H, Triazine CH), 7.76 (s, 1H, Pyrazole-CH₃), 3.27 (t, $J = 6.5$ Hz, 2H, S-CH₂-(CH₂)₇-CH₃), 2.44 (s, 3H, CH₃-pyrazole), 1.68–1.64 (m, 2H, S-CH₂-CH₂-C₇H₁₅), 1.41–1.30 (m, 2H, S-(CH₂)₂-CH₂-C₆H₁₃), 1.33–1.21 (m, 10H, S-(CH₂)₃-(CH₂)₅-CH₃), 0.91–0.86 (m, 3H, S-(CH₂)₈-CH₃). ESI MS (m/z): [M+H]⁺

at 333. EA (C₁₆H₂₄N₆S), calculated, %: C - 57.80, H - 7.28, N - 25.28, S - 9.64; obtained, %: C - 57.93, H - 7.26, N - 25.22, S - 9.67.

3-(Decylthio)-9-methylpyrazolo[1,5-d][1,2,4]triazolo[3,4-f][1,2,4]triazine (2.20)

White crystalline solid in 74% yield, m. p. (°C): 191 – 193. ¹H-NMR (400 MHz), δ (ppm): 8.95 (s, 1H, Triazine CH), 7.76 (s, 1H, Pyrazole CH), 3.25 (t, $J=6.5$ Hz, 2H, S-CH₂-C₉H₁₉), 2.45 (s, 3H, Pyrazole-CH₃), 1.73–1.64 (m, 2H, S-CH₂-CH₂-C₈H₁₇), 1.40–1.20 (m, 12H, S-(CH₂)₃-(CH₂)₆-CH₃), 0.89–0.84 (m, 3H, S-(CH₂)₉-CH₃). ESI MS (m/z): [M+H]⁺ at 347. EA (C₁₇H₂₆N₆S), calculated, %: C - 58.93, H - 7.56, N - 24.25, S - 9.25; obtained, %: C - 58.84, H - 7.57, N - 24.21, S - 9.23.

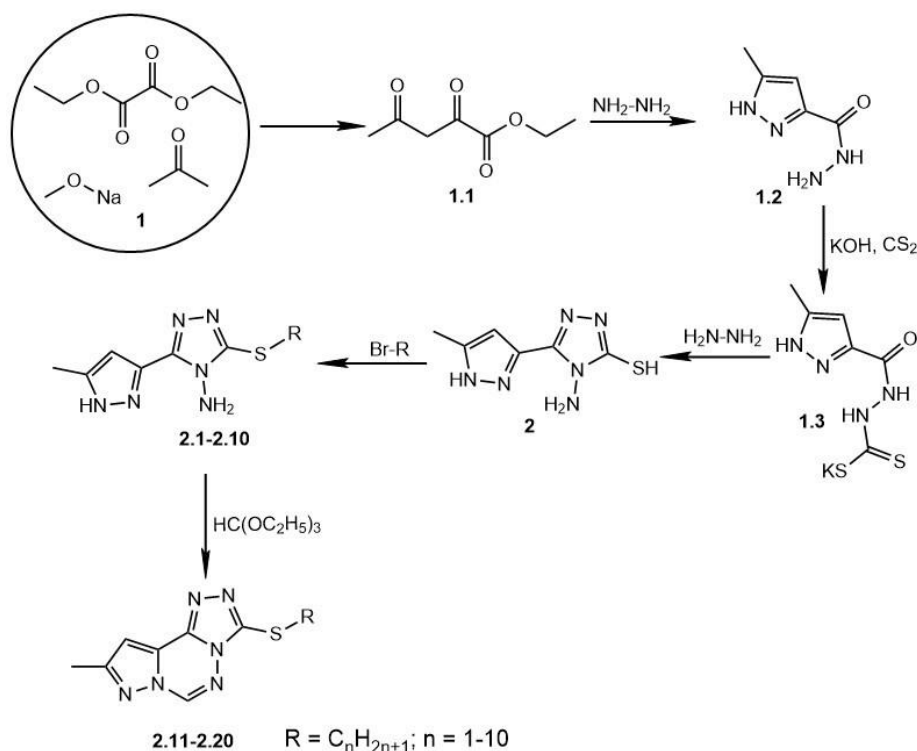


Figure 1. The scheme for the synthesis of target products of chemical transformation

The structure of all *S*-alkyl derivatives (2.11-2.20) was confirmed by physico-chemical methods, in particular by ¹H-NMR spectroscopy.

In the ¹H-NMR spectra of the final reaction products (2.11-2.20), the Hydrogen of the 1,2,4-triazine cycle forms a clear singlet signal, which has been registered at 8.96-8.92 ppm. The methine moiety of the pyrazole fragment forms a singlet at 7.76-7.73 ppm the methyl substitute of the pyrazole ring forms a three-proton singlet signal at 2.45-2.42 ppm.

The formation of *S*-alkyl derivatives is expected to be accompanied by the appearance of alkyl fragments in the aliphatic part of the proton signal spectrum. For example, in the spectrum of compound 2.11, a signal is recorded in the form of a singlet at 2.76 ppm, which is due to a methyl group bound to Sulfur.

The methylene group of the ethyl substitute of compound 2.12 is registered on the spectrum in the form of a quadruplet at 3.24 ppm the methyl fragment of this substitute forms a triplet at 1.32 ppm.

The propyl substituent of compound 2.13 contributes to the appearance on the spectrum of two triplets at 3.12 ppm and 1.07 ppm respectively, as well as a quadruplet at 1.78 ppm. Proton signals of methylene fragments of other compounds (2.14-2.20) are also recorded in the stronger magnetic field between 3.28-1.20 ppm. The elongation of the *S*-alkyl chain results in a small displacement in the proton' signals of CH₃-group to the stronger part of the field.

For example, the proton signals of the CH_3 group of the decyle substituent ($-(\text{CH}_2)_9-\text{CH}_3$) manifest as a multiplet in the range 0.89-0.84 ppm. Proton signals of most methylene fragments ($\text{CH}_2-\text{CH}_2-\text{C}_8\text{H}_{17}$, $-(\text{CH}_2)_3-(\text{CH}_2)_6-\text{CH}_3$) also appear as multiplets in the intervals of 1.73-1.64 ppm and 1.40-1.20 ppm, but they are difficult to differentiate between each other. At the same time, the proton signals of the methylene fragment, which is directly bound to the Sulfur ($\text{CH}_2-\text{C}_9\text{H}_{19}$), manifest as a triplet and are fixed in a weaker field at 3.25 ppm.

The mass spectra of compounds 2.11-2.20 contain peaks of molecular ions that correspond to the molecular weight. The quantitative deviation during the elemental analysis was within $\pm 0.3\%$.

Molecular Docking

The creation of new original drugs takes into account the use of a wide range of methods that can reveal the true level of biological potential of new molecules. Among such methods, one of the primary and main is molecular docking. This method makes it possible to reliably determine the biological target for binding to the ligand and helps to rationally approach the process of creating potential candidates for the drug substance [21,22].

Analyzing the similarity of the composition of the obtained substances to the structure of known drugs, it was decided to test the possibility of the effect of the studied substances on enzymes that are associated with the inflammatory process, antifungal activity and anti-cancer effect.

The study was based on modeling complexes with cyclooxygenase-2, lanosterol 14 α -demethylase, and receptor tyrosine kinase. These actions made it possible to successfully obtain the bond energy values of the studied ligand to the receptor protein and perform a visual assessment.

The results were evaluated in comparison with celecoxib, which has a pharmacophore pyrazole fragment similar to the synthesized compounds. It is a well-known fact that the nature of the interaction of celecoxib with the active COX-2 center is very diverse. This phenomenon is due to the fact that almost all structural fragments of celecoxib are involved in the interaction. The most important structural fragment that directly forms bonds with the hydrophilic "pocket" of COX-2 is the polar sulfamide group of celecoxib. An equally important role in the interaction is played by the conjugated $p-\pi$ system of pyrazole, which contacts the residues Ala A: 528 and Val A: 350 (Figure 2).

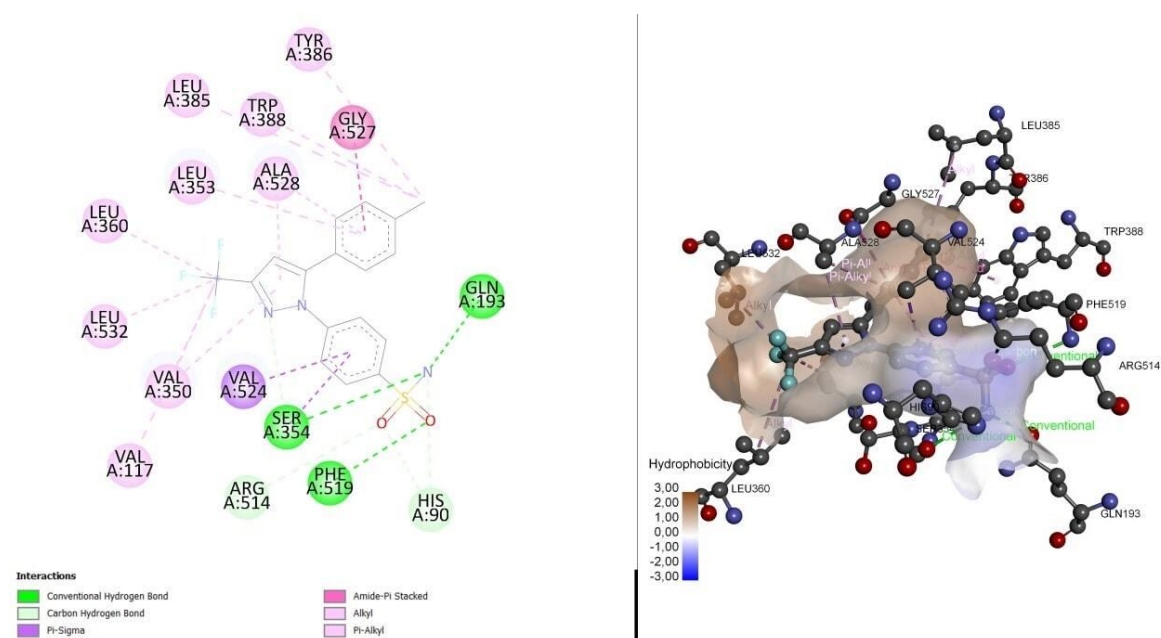


Figure 2. Visualization scheme for binding celecoxib to COX-2

Studies of the interactions of synthesized substances (2.11-2.20) with the active site of COX-2 helped to establish a certain level of similarity with celecoxib. The active participation of the thioalkyl residue in the formation of additional contacts with COX-2 was also demonstrated (Table 1).

Table 1. Main types of interactions between the studied compounds and amino acid residues of COX-2

	Nature of the amino acid residue
2.11	Ala A: 528, Leu A: 385, Phe A: 519, Met A: 523, Trp A: 388, Val A: 350, Val A: 524, Tyr A: 386, Val A: 117
2.12	Ala A: 528, Leu A: 353, Phe A: 519, Trp A: 388, Tyr A: 356, Val A: 350, Val A: 524, Leu A: 532, Val A: 117
2.13	Ala A: 528, Leu A: 353, Phe A: 519, Trp A: 388, Tyr A: 356, Leu A: 93, Val A: 89, Val A: 117
2.14	Ala A: 528, Trp A: 388, Leu A: 353, Phe A: 519, Tyr A: 386, Tyr A: 356, Val A: 350, Val A: 524, Val A: 117, Tyr A: 116
2.15	Ala A: 528, Tyr A: 386, Trp A: 388, Val A: 524, Val A: 350, Tyr A: 356, Val A: 117, Leu A: 93, Val A: 89, Tyr A: 116
2.16	Ala A: 528, Gly A: 527, Tyr A: 386, Trp A: 388, Leu A: 385, Val A: 524, Val A: 350, Tyr A: 356, Val A: 117, Leu A: 93, Tyr A: 116, Ser A: 531
2.17	Ala A: 528, Gly A: 527, Tyr A: 386, Trp A: 388, Leu A: 385, Val A: 524, Ser A: 531, Val A: 350, Tyr A: 356, Val A: 117, Leu A: 93, Val A: 89, Tyr A: 116
2.18	Ala A: 528, Leu A: 385, Val A: 350, Trp A: 349, Leu A: 532, Val A: 524, Tyr A: 386, Val A: 117, Tyr A: 116, Leu A: 93, Ile A: 113, Trp A: 100
2.19	Ala A: 528, Gly A: 527, Tyr A: 386, Leu A: 385, Trp A: 388, Phe A: 382, Val A: 524, Val A: 350, Tyr A: 356, Leu A: 93, Tyr A: 116, Val A: 117, Ile A: 113
2.20	Ala A: 528, Gly A: 527, Tyr A: 386, Phe A: 382, Leu A: 385, Trp A: 388, Val A: 524, Ser A: 531, Val A: 350, Leu A: 353, Tyr A: 356, Val A: 117, Leu A: 93, Tyr A: 116, Ile A: 113

For example, compound 2.11 performs the π - σ interaction using fragments Ala A: 528 and Val A: 350, to which 1,2,4-triazole and 1,2,4-triazine fragments are added. It helps to coordinate the ligand in the active center region and the π -alkyl interaction, which involves Leu A: 532 and Val A: 524 residues. And here the CH₃ group of pyrazole synthon makes a very significant contribution, and this is realized using Leu A: 353, Phe A: 519 and Trp A: 388. The hydrogen bond also makes a feasible contribution to the implementation of this interaction. And here the endocyclic Nitrogen atom of the triazole cycle and Tyr A: 356 actively help. The complicated complex of interactions with COX-2 π -S is enhanced by contact with the Tyr A: 356 residue and Van der Waals forces involving Gly A: 527, Ser A: 531 and Tyr A: 386.

A rise of C-atoms amount in the structure of the alkyl substituent contributed to a modest rise in the number of chemical bonds that are formed with amino acid residues. In this case, the qualitative and quantitative indicators of the interaction process were complex and complex in nature, but in most cases, it is the hydrophobic nature of the interaction (alkyl, π - σ and π -alkyl interactions) that prevails. For example, the thioethyl substitute (2.12) contributes to the formation of an alkyl type of interaction with the Val A: 117 residue. The thiopropyl fragment of compound 2.13 causes additional alkyl interactions involving Ala A: 528, Leu A: 93, and Val A: 89 residues. But at the same time, this process is compensated by an increase in the number of interactions with amino acid residues (Leu A: 353, Phe A: 519, Trp A: 388, Tyr A: 386), which occurs through the CH₃ group of the pyrazole ring. A rise in the size of the thioalkyl moiety to 5 carbon atoms (2.15) is again followed by a reduce the number of alkyl interactions with amino acid residues, which suggests a more pronounced engagement of the molecule with the enzyme binding place. However, simultaneously, the loss of intermolecular hydrogen chemical bonds is recorded, which is explained by an elongation of the hydrophobic moiety and a significant change in the orientation of the triazole fragment in the binding site. It is the Nitrogen atoms of the triazole cycle that are responsible for the formation of this type of chemical bond. It is also necessary to pay attention to the fact that S-alkyl substituted in a series of obtained substances with the number of

carbon atoms from 1 to 4 are additionally stabilized at the COX-2 π -S binding site by the interaction of the ligand with the amino acid residue Tyr A: 356 (2.11-2.14) (Figure 3).

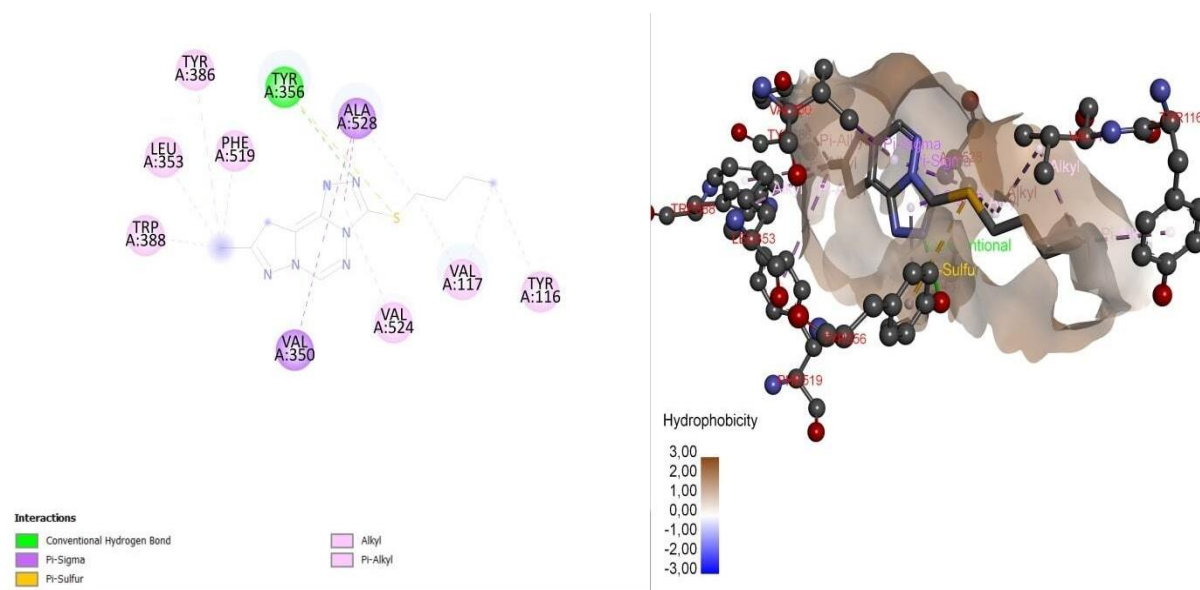


Figure 3. Visualization scheme for binding compound 2.14 to COX-2

The minimum free binding energy of the synthesized compounds to COX-2 is in the range of $-4.9 \dots -7.5 \text{ kcal} \times \text{mol}^{-1}$, which, together with the results of visualization of docking with this enzyme, does not allow us to confidently speak about the high probability of anti-inflammatory activity. However, some compounds (2.14-2.16) in the future would be interesting to study for anti-inflammatory activity *in vitro* and *in vivo* (Table 2).

Table 2. Energy metrics of the molecular engagement involving COX-2

№	$\epsilon_{\text{min}}, \frac{\text{kcal}}{\text{mol}}$	№	$\epsilon_{\text{min}}, \frac{\text{kcal}}{\text{mol}}$	№	$\epsilon_{\text{min}}, \frac{\text{kcal}}{\text{mol}}$
2.11	-6.4	2.15	-7.1	2.19	-4.9
2.12	-6.6	2.16	-5.9	2.20	-4.9
2.13	-7.1	2.17	-5.2	<i>Celecoxib</i>	-13.4
2.14	-7.5	2.18	-4.9		

* ϵ_{min} - The minimum energy of complex formation.

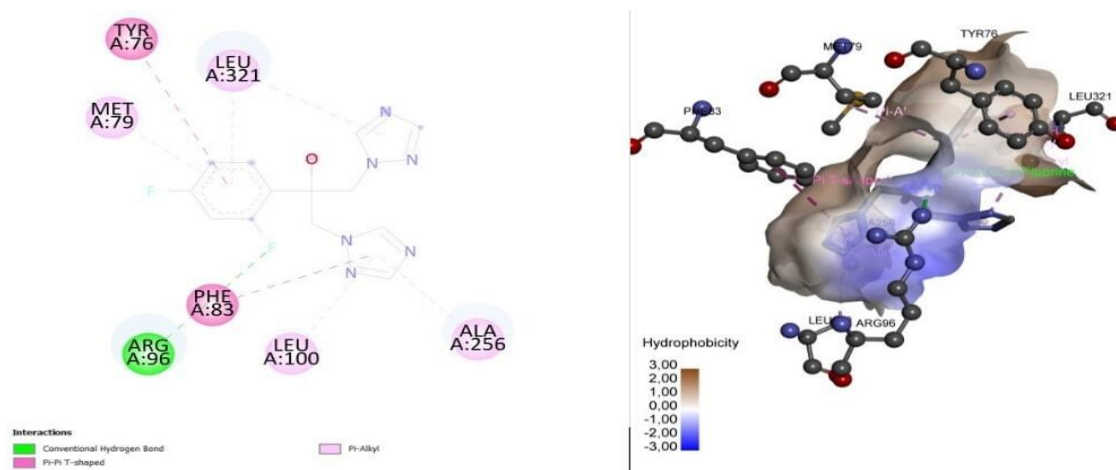
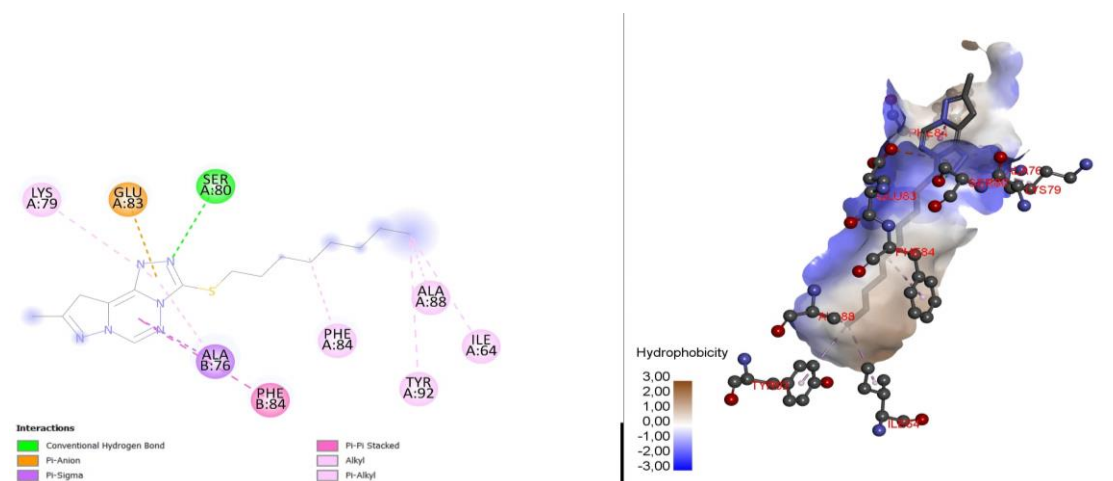
The vast majority of known antifungal drugs have one or more heterocyclic fragments in their structure. The most well-known such fragments include 1,2,4-triazole, imidazole, and pyridine. This type of interaction (Figure 4) contributes to the loss of lanosterol 14α -demethylase activity and disruption of the synthesis of ergosterol, which is a structural component of the fungal cell membrane.

With a view to assessing the possible influence of the obtained ligands (2.11-2.20) on the activity of this enzyme, docking studies were conducted with visualization of the results. The synthesized compounds have the ability to affect lanosterol 14α -demethylase, which is realized due to a set of certain types of interactions with the active center of this enzyme (Table 3).

For example, alkyl substituents in the structure of synthesized substances (2.11-2.20) actively affect the formation of hydrophobic interactions that occur with the participation of the corresponding fragments of amino acids of the specified demethylase (Ala A: 76, Ala A: 88, Ile A: 64, Phe A: 84, Tyr A: 92) (Figure 5).

Table 3. Main types of interactions between the studied compounds and amino acid residues of lanosterol 14 α -demethylase

	Nature of the amino acid residue
2.11	Ala A: 88, Ile A: 64, Phe A: 84, Lys A: 79, Lys B: 79
2.12	Ala A: 76, Ala A: 88, Lys A: 79, Lys B: 79, Ser A: 80, Phe A: 84, Tyr A: 92, Ile A: 64
2.13	Ala A: 76, Ala B: 76, Ala A: 88, Ser A: 80, Ser B: 80, Phe A: 84
2.14	Ala A: 76, Ala B: 76, Ala A: 88, Ser A: 80, Ser B: 80, Phe A: 84, Phe B: 84, Ile A: 64, Tyr A: 92, Lys B: 79
2.15	Ala A: 76, Ala B: 76, Ala A: 88, Glu A: 83, Ile A: 64, Ser A: 80, Ser B: 80, Phe A: 84, Tyr A: 92
2.16	Ala A: 76, Ala B: 76, Ala A: 88, Glu A: 83, Phe B: 84, Phe A: 84, Tyr A: 92, Ile A: 64
2.17	Ala A: 76, Ala A: 88, Glu A: 83, Phe B: 84, Phe A: 84, Ser A: 80, Tyr A: 92, Ile A: 64
2.18	Ala A: 76, Ala A: 88, Glu A: 83, Lys A: 79, Ser A: 80, Phe B: 84, Phe A: 84, Tyr A: 92, Ile A: 64
2.19	Ala A: 76, Ala A: 88, Asn A: 87, His A: 73, Ile A: 64, Phe A: 84, Ile A: 64
2.20	Ala A: 76, Ala A: 88, Ile A: 64, Phe A: 84, Phe B: 84, Ile A: 64, Tyr A: 92

**Figure 4.** Imaging scheme for binding fluconazole to lanosterol 14 α -demethylase**Figure 5.** Imaging scheme for binding compound 2.18 to lanosterol 14 α -demethylase

Attention is also drawn to the π -anionic interactions that are formed with the participation of triazole and triazine cycles upon contact with Glu A: 83. Additionally, ligand-protein complexes are stabilized by the formation of intermolecular hydrogen chemical bonds. This type of chemical bond is

formed with the direct participation of triazole synthon nitrogen in interaction with the Ser A: 80 residue, as well as with the participation of triazine nitrogen in the process of contact with the Asn B: 87 fragment. The triazine fragment in the structure of synthesized compounds plays one of the key roles in the formation of interactions with lanosterol 14 α -demethylase due to the stacking interaction with the amino acid residue Phe B: 84. The largest number of interactions is recorded for compound 2.18. The occurrence of such a large number of interactions allows us to predict a positive effect on the possibility of antifungal activity. Probably, the structure of this compound makes it possible to occupy the most favorable position in the active site of lanosterol 14 α -demethylase. But despite this fact, compounds 2.19 and 2.20 have the best indicator of the binding energy of the ligand-receptor complex (Table 4).

The value of the minimum free binding energy of the synthesized compounds to lanosterol 14 α -demethylase is in the range of -6.1 ... -9.5 kcal \times mol⁻¹ (Table 4). Taking into account these values and the results of docking imaging, we can conclude that an extended study of certain compounds (2.19, 2.20) for antifungal activity is promising.

Table 4. Energy metrics of the molecular engagement involving lanosterol 14 α -demethylase

N_{c}	$\epsilon_{\text{min}}, \frac{\text{kcal}}{\text{mol}}$	N_{c}	$\epsilon_{\text{min}}, \frac{\text{kcal}}{\text{mol}}$	N_{c}	$\epsilon_{\text{min}}, \frac{\text{kcal}}{\text{mol}}$
2.11	-6.1	2.15	-8.0	2.19	-9.0
2.12	-6.9	2.16	-8.2	2.20	-9.5
2.13	-7.4	2.17	-8.1	<i>Fluconazole</i>	-10.9
2.14	-8.1	2.18	-8.4		

* ϵ_{min} - The minimum energy of complex formation.

The structure of crizotinib, a well-known anti-cancer drug, includes, among other things, a fragment of pyrazole. Therefore, among other things, it was interesting to test the possibility of the effect of synthesized substances on the crizotinib-dependent enzyme.

Receptor tyrosine kinase was chosen as the model enzyme, an increase in the activity of which is associated with the development of certain types of cancer. In line with the outcomes of molecular docking, the specified drug is captured in the receptor tyrosine kinase binding site using H-bonds that are formed between the N-atom of heterocyclic fragments of the crizotinib molecule and the residues of the Met A: 1199, Glu A: 1197 enzyme.

Additional stabilization of crizotinib at the binding site occurs with the active help of alkyl and π -alkyl interactions involving Ala A: 1148 and Leu A: 1122 (Figure 6). A crucial part is also carried out by the π - σ interaction, that are being implemented through to Leu A: 1256. Attention should also be paid to the spatial interaction of Chlorine and Fluorine with Asn A: 1254 and Gly A: 1269.

Trends in the amount for C-atoms within the structure of the thioalkyl substitute of synthesized compounds actively determine the nature and number of amino-acid snippets in the tyrosine kinase binding site, which will be involved in interaction with the ligand (Figure 7).

The synthesized compounds (2.11-2.20) can form the following types of interactions with the active site of tyrosine kinase: alkyl-alkyl hydrophobic interaction of the thioalkyl substitute with residues Leu A: 1196, Leu A: 1256 and Lys A: 1150; π -alkyl – with residues Ala A: 1148 and Leu A: 1256, π - σ - with residue Gly A: 1202 (Table 5).

Interactions that enhance contact with the enzyme can be noted C-H interaction. A lengthening of the alkyl chain leads in some cases to an increase in the number of additional hydrophobic interactions, for example, with the amino acid residue Ile A: 1171 (with the methyl group of the octyl and nonyl substituent). The transition to decyl substitute is accompanied by a decrease in the number of amino-acid pieces of the active zone of tyrosine kinase, which interact with the ligand and, in turn, is characterized exclusively by an alkyl interaction.

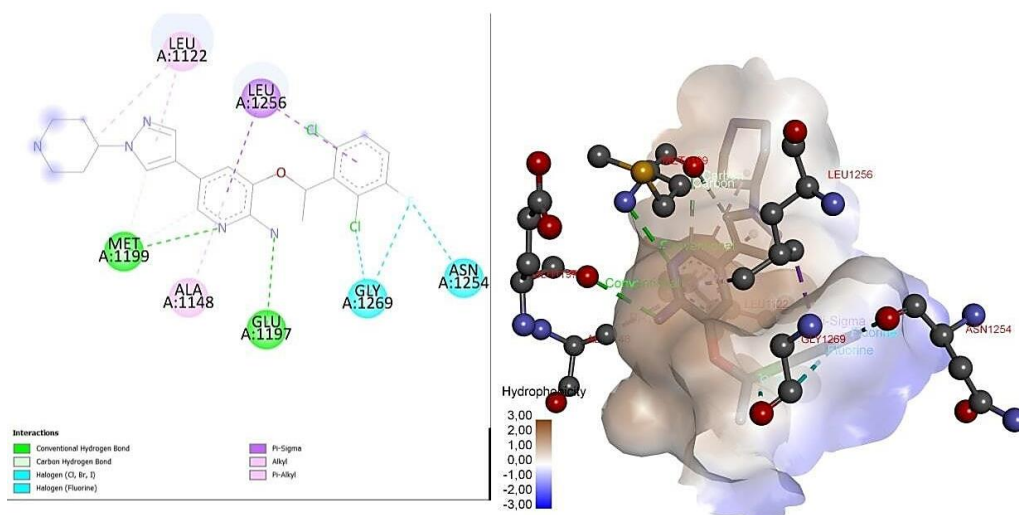


Figure 6. Imaging scheme for the binding of crizotinib to tyrosine kinase

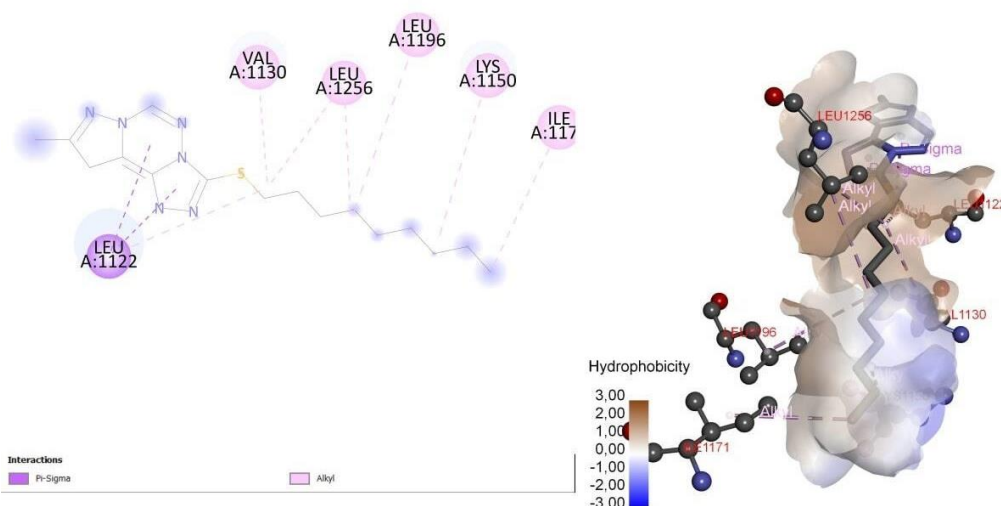


Figure 7. Imaging scheme for the binding of compound 2.19 to tyrosine kinase

Table 5. Main types of interactions between the studied compounds and amino acid residues of receptor tyrosine kinase

	Nature of the amino acid residue
2.11	Ala A: 1148, Leu A: 1122, Leu A: 1196, Leu A: 1256, Val A: 1130
2.12	Ala A: 1148, Leu A: 1122, Leu A: 1196, Leu A: 1256, Val A: 1130
2.13	Ala A: 1148, Leu A: 1122, Leu A: 1196, Leu A: 1256, Val A: 1130
2.14	Ala A: 1148, Leu A: 1122, Leu A: 1256, Lys A: 1150, Val A: 1130
2.15	Ala A: 1148, Ala A: 1200, Leu A: 1122, Leu A: 1196, Leu A: 1256, Val A: 1130
2.16	Ala A: 1148, Gly A: 1202, Leu A: 1122, Leu A: 1256, Leu A: 1196, Lys A: 1150
2.17	Ala A: 1148, Leu A: 1122, Leu A: 1256, Leu A: 1196, Lys A: 1150, Ile A: 1171
2.18	Leu A: 1122, Leu A: 1196, Leu A: 1256, Met A: 1199, Val A: 1130, Lys A: 1150
2.19	Leu A: 1122, Leu A: 1196, Leu A: 1256, Lys A: 1150, Ile A: 1171, Val A: 1130
2.20	Leu A: 1122, Leu A: 1196, Leu A: 1256, Lys A: 1150, Val A: 1130

The test substances are in contact with the receptor tyrosine kinase with a minimum free binding energy of -6.0 to -7.6 kcal \times mol⁻¹ (Table 6).

Table 6. Energy metrics of the molecular engagement with the receptor tyrosine kinase

№	$\epsilon_{\min}, \frac{kcal}{mol}$	№	$\epsilon_{\min}, \frac{kcal}{mol}$	№	$\epsilon_{\min}, \frac{kcal}{mol}$
2.11	-6.0	2.15	-6.3	2.19	-7.5
2.12	-6.2	2.16	-7.5	2.20	-7.6
2.13	-6.4	2.17	-7.5	<i>Crizotinib</i>	-10.8
2.14	-6.6	2.18	-7.4		

* ϵ_{\min} - The minimum energy of complex formation.

Thus, docking studies of the synthesized thioalkyl-substituted of 9-methylpyrazolo[1,5-*d*][1,2,4]-triazolo[3,4-*f*][1,2,4]triazine (2.11-2.20) indicate a low the probability of impact on receptor tyrosine kinase of these ligands.

A series of mercaptoalkyl-9-methylpyrazolo[1,5-*d*][1,2,4]triazolo[3,4-*f*][1,2,4]triazines has been successfully synthesized. The structure of the synthesized substances is proven by modern methods of analysis. The conducted molecular docking made it possible to identify a number of promising compounds for subsequent research of anti-inflammatory and fungicidal activity.

The results of studies have shown that the synthesized compounds show the greatest affinity for lanosterol 14 α -demethylase. The obtained values of the predicted free binding energy with the active center of the specified enzyme allowed us to determine the most promising compound for further research, which turned out to be substance 2.20.

ACKNOWLEDGEMENTS

The authors would like to thank A. Voskoboynik (ZSMU, Zaporizhzhia, Ukraine) considerable support during the preparation this article.

AUTHOR CONTRIBUTIONS

Concept: S.F., A.G.; Design: S.F., A.G.; Control: A.G.; Sources: S.F., A.G.; Materials: S.F., T.B.; Data Collection and/or Processing: S.F., Y.Z.; Analysis and/or Interpretation: S.F., A.G.; Literature Review: A.G.; Manuscript Writing: S.F., A.G.; Critical Review: Y.Z., T.B.; Other: -

CONFLICT OF INTEREST

The authors declare that there is no real, potential, or perceived conflict of interest for this article.

ETHICS COMMITTEE APPROVAL

The authors declare that the ethics committee approval is not required for this study.

REFERENCES

- Boraei, A.T.A., Sarhan, A.A.M., Yousuf, S., Barakat, A. (2020). Synthesis of a new series of nitrogen/sulfur Heterocycles by linking four rings: Indole; 1,2,4-triazole; pyridazine; and quinoxaline. *Molecules*, 25(3), 450. [\[CrossRef\]](#)
- Shcherbyna, R., Panasenko, O., Polonets, O., Nedorezaniuk, N., Duchenko, M. (2021). Synthesis, antimicrobial and antifungal activity of ylidenhydrazides of 2-((4-R-5-R₁-4*H*-1,2,4-triazol-3-yl)thio)acetaldehydes. *Journal of Faculty of Pharmacy of Ankara University*, 45(3), 504-514. [\[CrossRef\]](#)
- Frolova, Y., Kaplaushenko, A., Nagornaya, N. (2020). Design, synthesis, antimicrobial and antifungal activities of new 1,2,4-triazole derivatives containing 1*H*-tetrazole moiety. *Journal of Faculty of Pharmacy of Ankara University*, 44(1), 70-88. [\[CrossRef\]](#)

4. Samelyuk, Y.G., Kaplaushenko, A.G. (2014). Synthesis of 3-alkylthio(sulfo)-1,2,4-triazoles, containing methoxyphenyl substituents at C⁵atoms, their antipyretic activity, propensity to adsorption and acute toxicity. *Journal of Chemical and Pharmaceutical Research*, 6(5), 1117-1121.
5. Aggarwal, R., Sumran, G. (2020). An insight on medicinal attributes of 1,2,4-triazoles. *European Journal of Medicinal Chemistry*, 205, 112652. [[CrossRef](#)]
6. Zaher, N.H., Mostafa, M.I., Altaher, A.Y. (2020). Design, synthesis and molecular docking of novel triazole derivatives as potential CoV helicase inhibitors. *Acta Pharmaceutica*, 70(2), 145-159. [[CrossRef](#)]
7. Vanjare, B.D., Mahajan, P.G., Dige, N.C., Raza, H., Hassan, M., Han, Y., Lee, K.H. (2020). Novel 1,2,4-triazole analogues as mushroom tyrosinase inhibitors: synthesis, kinetic mechanism, cytotoxicity and computational studies. *Molecular Diversity*, 25, 2089-2106 [[CrossRef](#)]
8. Safonov, A. (2020). Method of synthesis novel N'-substituted 2-((5-(thiophen-2-ylmethyl)-4*H*-1,2,4-triazol-3-yl)thio)acetohydrazides. *Journal of Faculty of Pharmacy of Ankara University*, 44(2), 242-252. [[CrossRef](#)]
9. Safonov, A., Nevmyvaka, A., Panasenko, O., Knysh, Y. (2021). Microwave synthesis of 3- and 4-substituted-5-((3-phenylpropyl)thio)-4*H*-1,2,4-triazoles. *Journal of Faculty of Pharmacy of Ankara University*, 45(3), 457-466. [[CrossRef](#)]
10. Simurova, N.V., Maiboroda, O.I. (2021) Antiviral activity of 1,2,4-triazole derivatives (microreview). *Chemistry of Heterocyclic Compounds*, 57, 420-422. [[CrossRef](#)]
11. Singla, N. (2020). Synthetic and medicinal attributes of 1,2,4-triazole derivatives, *Annals of Tropical Medicine & Public Health*, 23(14), SP231541.
12. Hotsulia, A.S., Fedotov, S.O. (2019). Synthesis, structure and properties of N-R-2-(5-(5-methyl-1*H*-pyrazole-3-yl)-4-phenyl-4*H*-1,2,4-triazole-3-ylthio)acetamides. *Current Issues in Pharmacy and Medicine: Science and Practice*, 12(1), 4-9. [[CrossRef](#)]
13. Fedotov, S.O., Hotsulia, A.S. (2021). Synthesis and properties of S-derivatives of 4-amino-5-(5-methylpyrazol-3-yl)-1,2,4-triazole-3-thiol. *Current Issues in Pharmacy and Medicine: Science and Practice*, 14(3), 268-274. [[CrossRef](#)]
14. Karrouchi, K., Chemlal, L., Taoufik, J., Cherrah, Y., Radi, S., El Abbes Faouzi, M., Ansar, M. (2016). Synthesis, antioxidant and analgesic activities of Schiff bases of 4-amino-1,2,4-triazole derivatives containing a pyrazole moiety. *Annales Pharmaceutiques Françaises*, 74(6), 431-438.
15. Varynskyi, B., Kaplaushenko, A., Parchenko, V. (2018). Electrospray ionization mass spectrometry fragmentation pathways of salts of some 1,2,4-triazolylthioacetate acids, the active pharmaceutical ingredients. *The Asian Journal of Pharmaceutical and Clinical Research*, 10, 303-312. [[CrossRef](#)]
16. Karpun, Y.O., Karpenko, Y.V., Parchenko, M.V., Bihdan, O.A. (2020). Molecular docking and bioavailability of S-alkyl derivatives 5-(3-fluorophenyl)-, 5-(5-bromofuran-2-yl)- and -(((3-(pyridin-4-yl)-1*H*-1,2,4-triazole-5-yl)thio)methyl)-4-methyl-4*H*-1,2,4-triazole *in silico* methods. *Current Issues in Pharmacy and Medicine: Science and Practice*, 13(1), 38-45. [[CrossRef](#)]
17. El Bakri, Y., Marmouzi, I., El Jemli, M., Anouar, E.H., Karthikeyan, S., Harmaoui, A., Faouzi, M.E.A., Mague, J.T., Essassi, E.M. (2019). Synthesis, biological activity and molecular modeling of a new series of condensed 1,2,4-triazoles. *Bioorganic Chemistry*, 92, 103193. [[CrossRef](#)]
18. Protein Data Bank, [pdb.http://www.rcsb.org/pdb/home/home.do](http://www.rcsb.org/pdb/home/home.do)
19. MarvinSketch version 17.21.0, ChemAxon Retrieved from <https://chemaxon.com/>
20. Trott O., Olson A.J. (2020). AutoDock Vina: improving the speed and accuracy of docking with a new scoring function, efficient optimization, and multithreading. *Journal of Computational Chemistry*, 31, 455-461.
21. Ghanaat, J., Khalilzadeh, M.A., Zareyee, D. (2020). Molecular docking studies, biological evaluation and synthesis of novel 3-mercapto-1,2,4-triazole derivatives. *Molecular Diversity*, 25(1), 223-232. [[CrossRef](#)]
22. El-Reedy, A.A.M., Soliman, N.K. (2020). Synthesis, biological activity and molecular modeling study of novel 1,2,4-triazolo[4,3-*b*][1,2,4,5]tetrazines and 1,2,4-triazolo[4,3-*b*][1,2,4]triazines. *Scientific Reports*, 10, 6137. [[CrossRef](#)]